AJNR

Pre- and postoperative MR evaluation of stereotactic pallidotomy.

M C Cohn, P A Hudgins, S K Sheppard, P A Starr and R A Bakay

AJNR Am J Neuroradiol 1998, 19 (6) 1075-1080
http://www.ajnr.org/content/19/6/1075

AJNR Am J Neuroradiol 19:1075–1080, June 1998

Pre- and Postoperative MR Evaluation of Stereotactic Pallidotomy

Michael C. Cohn, Patricia A. Hudgins, Scott K. Sheppard, Phillip A. Starr, and Roy A. E. Bakay

PURPOSE: **Stereotactic pallidotomy, which has evolved as a result of technological advances in high-resolution MR imaging and microelectrode electrophysiological recording, is becoming a major form of treatment for patients with Parkinson disease in whom medical therapy has failed. We describe the location and appearance of the pallidotomy lesion on high-resolution MR images.**

METHODS: **MR images in 83 patients (60 men and 23 women) who underwent stereotactic pallidotomy were reviewed retrospectively. The prepallidotomy screening study included standard spin-echo and gradient-echo sequences. After placement of a stereotactic headframe, volume-acquisition T1-weighted spoiled gradient-echo images were acquired for target localization in the posteroventral internal globus pallidus. One to three days after the pallidotomy, volume-acquisition T1-weighted and standard spin-echo sequences were obtained. In 16 patients, turbo spin-echo inversion recovery images also were obtained before and after surgery. The diameter, signal intensity, and location of the lesions relative to the midcommissural point and the intercommissural line were noted.**

RESULTS: **The average lesion volume was 118 mm^3 while that of the lesion-edema complex was 420 mm^3. The midportion of the lesion was located on average 3.5 mm anterior to the midcommissural point, 21 mm lateral to the middle of the third ventricle, and 1.2 mm inferior to the intercommissural line. Signal intensity of the lesions varied, but all had a rim of edema. Forty-two patients had edema extending into the optic tract, four had increased signal in the ipsilateral basal ganglia on T2-weighted images, and seven had hemorrhage involving the ipsilateral caudate, internal capsule, and putamen. All patients experienced some improvement in contralateral bradykinesia, rigidity, and dystonia.**

CONCLUSION: **The acute pallidotomy lesion is invariably located within the posteroventral internal globus pallidus, is usually hyperintense centrally on T1-weighted and turbo spin-echo inversion recovery MR images, and has a thin rim of edema. Edema extending into the ipsilateral optic tract was a common finding, but this series of patients evinced no visual changes.**

Parkinson disease, first described in 1817 by James Parkinson, is one of the most common diseases of the extrapyramidal motor system. It is a disorder of middle or late life, with a gradual progression and prolonged course. The cardinal clinical signs are tremor, rigidity, bradykinesia, and gait disorder. Eventually, patients may become so incapacitated that they require custodial care (1). The pathophysiology and biology of Parkinson disease are complex. The globus pallidus is made up of an internal segment (GPi) and an external segment (GPe) separated by the lamina medullaris medialis (Fig 1). The posteroventral portion of the GPi (pvGPi), the target, makes up a significant part of the basal ganglia thalamocortical (motor) circuit, and is responsible for motor disturbances in Parkinson disease (2–5). Surgical treatment of Parkinson disease has evolved over 60 years. Early surgical developments led to stereotactic neurosurgical intervention and eventually to selective GPi destruction. With the advent of dopamine replacement therapy, surgical interventions were, for the most part, replaced by medical treatment. However, technological advances in GPi lesion localization, including both high-resolution MR imaging and microelectrode electrophysiological recording techniques, have renewed interest in stereotactic pallidotomy. The pur-

Received May 1, 1997; accepted after revision December 11.

Presented at the annual meeting of the American Society of Neuroradiology, Toronto, May 1997.

From the Departments of Radiology (M.C.C., P.A.H., S.K.S.) and Neurosurgery (P.A.S., R.A.E.B.), Emory University, Atlanta, GA, and Philips Medical Systems, Shelton, CT (S.K.S.).

Address reprint requests to Patricia A. Hudgins, MD, Department of Radiology, Section of Neuroradiology, Emory University School of Medicine, 1364 Clifton Rd, NE, Atlanta, GA 30322.

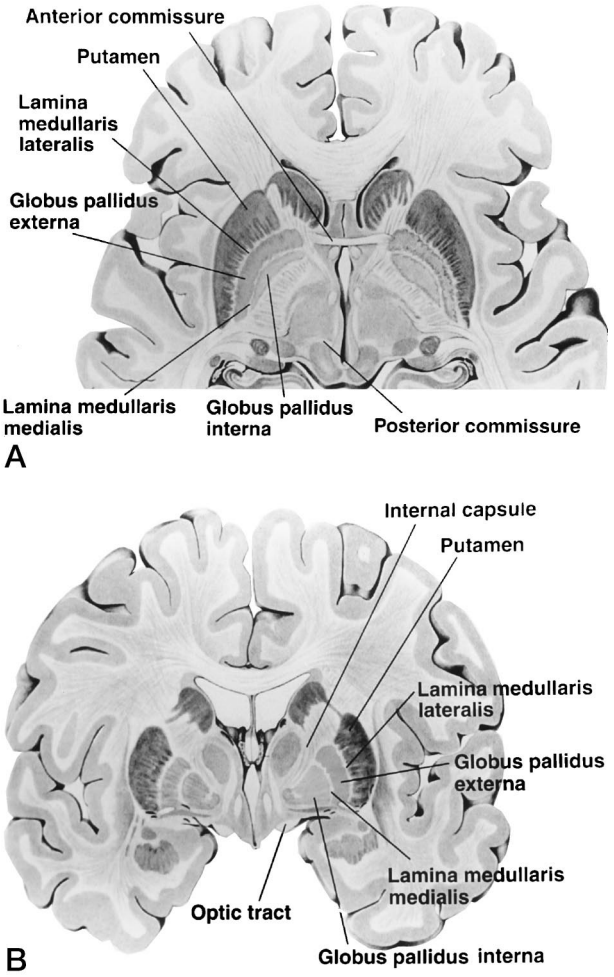

FIG 1. Anatomy of the globus pallidus. Axial (*A*) and coronal (*B*) diagrammatic depiction of the globus pallidus and surrounding structures. Note the lamina medullaris medialis separating the globus pallidus interna from the globus pallidus externa.

pose of this article is to discuss the role and method of pre- and postoperative MR imaging in stereotactic pallidotomy and to describe the expected location and appearance of the stereotactically placed pvGPi lesion, including its size and signal intensity on MR images.

Methods

The study population consisted of 83 patients (60 men and 23 women), ranging in age from 25 to 84 years (average age, 58 years). The criterion for surgical pallidotomy included moderate to advanced idiopathic Parkinson disease, as signified by two of the four cardinal signs and by decreasing benefit from dopamine replacement therapy. All MR examinations were reviewed retrospectively by a neuroradiologist and a general radiologist. Three separate MR examinations were performed for each patient, including a screening preoperative study, an immediate preoperative study with a stereotactic headframe in place, and a postoperative study within 48 hours of surgery. All antiparkinson medications were withheld after midnight prior to the preoperative MR examination in order to reduce drug-induced dyskinesias and to allow the manifestation of parkinsonian motor signs and their clinical assessment in the "off" state during lesion formation. The use of sedating drugs was

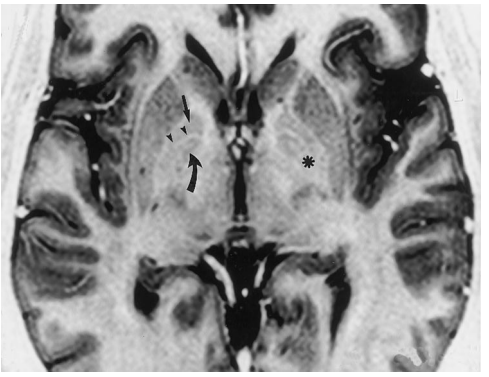

FIG 2. Turbo spin-echo IR (3000/40/4) axial MR image shows the site of the pallidotomy in the posteroventral GPi (*asterisk*). Globus pallidus interna (*curved arrow*), globus pallidus externa (*straight arrow*), and lamina medullaris medialis (*arrowheads*) are also shown.

minimized and aspirin was discontinued at least 1 week before the procedure.

The preoperative screening MR study was performed within 1 week before the pallidotomy procedure to assess for signs of secondary parkinsonism, such as lacunar infarction or lesions that might affect the decision to perform pallidotomy, such as extraaxial collections, severe atrophy, or hydrocephalus. Imaging was performed on a 1.5-T magnet and included conventional T1-weighted (649/15/1 [TR/TE/excitations]) sequences, fast spin-echo T2-weighted sequences (5000/100) with an echo train length of five, and gradient-echo (GRE) sequences (750/50) with a flip angle of 90° sensitive for magnetic susceptibility and iron deposition.

Using our stereotactic system, the neurosurgeon placed the headframe (Leksell series G) on the morning of surgery. Two plugs fit into the external auditory canals, aligning the frame with the axes orthogonal to the midsagittal plane of the brain. The anteroposterior axis of the frame was aligned with the infraorbital meatal line. When the axial images were made parallel to the frame, the anterior and posterior commissures and therefore the anterior-posterior commissure (AC-PC) line, an imaginary line drawn from the anterior to posterior commissure, were usually on the same axial image (6).

Initially, a spoiled GRE volume-acquisition sequence was acquired in the coronal plane for target localization. Parameters were 33/11/2, a flip angle of 35°, a voxel size of 1.0 mm^3, an angle through the AC-PC line, and localized shimming; time of acquisition was 12 minutes. More recently, a newly developed turbo spin-echo inversion recovery (IR) sequence was used, with parameters of 3000/40/5, inversion time of 200, multisection acquisition, 256 × 512 matrix, and 2-mm section thickness with no intersection gap. In both sequences the axial and coronal planes were used to establish the target coordinates. The stereotactic target, the pvGPi, was selected on the axial image passing through the AC-PC line at the point where the medial edge of the posterior GPi meets the internal capsule. The target, on the coronal image that passes through the mid AC-PC point, was selected at the inferior margin of the GPi superior to the lateral edge of the optic tract (7, 8) (Fig 2).

After the imaging studies were completed, the patient was transferred to the operating room, where a 10-mm burr hole was made anterior to the coronal suture and a platinum-iridium microelectrode was introduced into the brain with the trajectory in a parasagittal plane at an angle of 30° anterior to the perpendicular from the AC-PC line. The boundaries of the GPi and pvGPi were determined on the basis of the characteristic neuronal discharge frequencies and patterns. The optic tract was identified by light-induced axonal discharges. After the pallidal target was mapped with three to five microelectrode tracks, the microelectrode was replaced with a lesioning

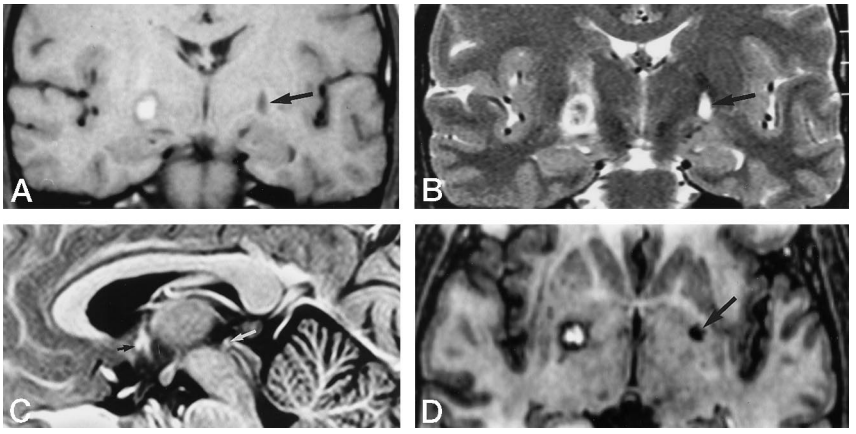

FIG 3. MR images 24 hours after right-sided pallidotomy. Note site of previous pallidotomy (on left) done 1 year earlier (*arrow, A B, and D*).

A, Coronal T1-weighted spin-echo (649/15/1) MR image shows hyperintense central portion surrounded by thin rim of low signal intensity, most likely representing edema. The older lesion on the left is smaller and nearly isointense with CSF.

B, Coronal T2-weighted fast spin-echo (5000/100/5) MR image shows hypointense central portion with a thin rim of hyperintense edema. As in *A*, the older lesion is smaller and homogeneously isointense with CSF.

C, Midline sagittal image obtained postoperatively shows anterior (*black arrow*) and posterior (*white arrow*) commissures. This image was used to locate the AC-PC line and to plan the angle of axial reformatting to best depict the AC-PC line on a single axial image.

D, Axial T1-weighted volume-acquisition spoiled GRE image (33/11) with a flip angle of 35° angled through the AC-PC line. Signal intensities are similar to those in *A*.

probe. Visual field and motor testing was carried out repeatedly during lesion formation.

One to three days after the pallidotomy procedure, a follow-up MR examination was done, including GRE volume-acquisition sequences (the matrix was 256 × 204 and the voxel size was 0.90 × 1.13 × 1.0 mm) for optimal T1 contrast and resolution, and conventional T1- and T2-weighted fast spin-echo sequences, described previously, in the coronal, axial, and sagittal planes. A turbo spin-echo IR sequence was obtained in the last 16 patients studied.

Both pre- and postoperative images were reviewed with a consensual approach by a neuroradiologist and a general radiologist. Motion artifacts were graded as none, mild, or severe. Measurements were made from film using a hand-held caliper.

Results

Findings on preoperative MR examinations were normal in 72 of the 83 patients. Most patients had several small dilated perivascular spaces within the basal ganglia, a finding considered normal. The abnormal findings in the 11 remaining patients included focal white matter ischemic lesions (n = 6), diffuse periventricular white matter changes (n = 2), generalized volume loss without focal lesions (n = 2), and a small left-sided parietal parafalcine meningioma (n = 1). Pallidotomies were done on the right side in 27 patients, on the left side in 54, and bilaterally in two cases. The side of the pallidotomy was determined on the basis of severity of symptoms in the contralateral body. The two patients who underwent bilateral procedures had severe bilateral symptoms. All patients experienced some immediate relief of symptoms, including contralateral bradykinesia, rigidity, and dystonia.

MR examinations obtained both preoperatively and on the day of surgery were without significant motion artifacts. Postoperative studies in eight of the 83 patients (imaged 1 to 3 days after the pallidotomy procedure) had at least one imaging sequence that was degraded by motion artifacts; however, all studies were considered to be of diagnostic quality.

The pallidotomy lesion had a rim of signal intensity that differed from the central portion. Signal intensity of the central portion of the pallidotomy lesion on T1-weighted spin-echo and GRE images was hyperintense (n = 82) or isointense (n = 3) relative to gray matter (Fig 3). This was considered the surgical lesion. On T1-weighted images, a rim of surrounding hypointensity was seen in each case. T2-weighted fast spin-echo images showed a hypointense center with a hyperintense rim (n = 85). The rim, therefore, was hypointense on T1-weighted images and hyperintense on T2-weighted images, most likely due to edema (Fig 3). In the 16 patients imaged with a turbo spin-echo IR sequence, the pallidotomy site contained a hyperintense center and a hypointense rim, characteristic of edema (Fig 4).

The average diameter of the pallidotomy lesion measured 5 mm (SD = 1.4) in the transverse dimension, 6 mm (SD = 1.5) in the anteroposterior dimension, and 7 mm (SD = 1.6) in the craniocaudal dimension. The volume of the pallidotomy lesions ranged from 52 to 264 mm^3, with the average measuring 118 mm^3 (SD = 57). The average diameter of the pallidotomy lesion-edema complex measured 8.6 mm (SD = 1.5) in the transverse dimension, 9.7 mm (SD = 1.4) anteroposteriorly, and 10.2 mm (SD = 1.6) craniocaudally. The volume of the pallidotomy lesion-edema complex ranged from 164.2 to 706 mm^3, with the average measuring 420 mm^3 (SD = 142.9).

The midportion of the lesions was located on average 3.5 mm (range, 0–6 mm; SD = 1.5) anterior to the midcommissural point, 21 mm (range, 17–25 mm; SD = 1.6) lateral to the middle of the third ventricle, and 1.2 mm (range, 0–3 mm; SD = 1.1) inferior to the midcommissural line.

Each postpallidotomy MR image showed a frontal burr hole, three to five probe tracts with minimal associated edema, and a small amount of pneumocephalus. In 42 of the 83 patients a pattern of high signal intensity was seen on the T2-weighted images and marked hypointensity was noted on the GRE sequences extending into the ipsilateral optic tract (Fig 5). No field cuts were apparent on gross confrontational examination. Four patients had increased sig-

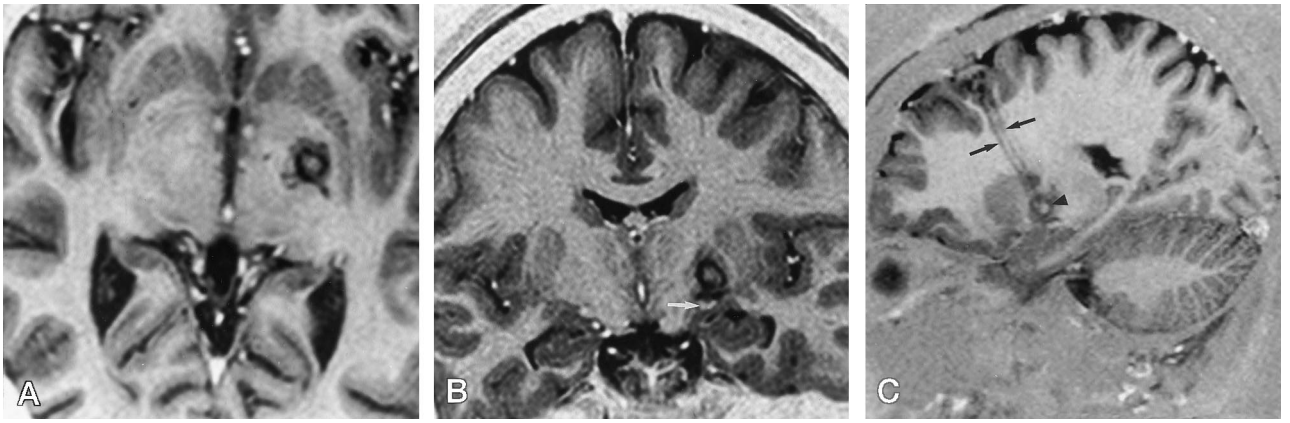

FIG 4. Turbo spin-echo IR (3000/40/4) MR images 24 hours after left-sided pallidotomy.
A, Axial high-resolution image shows a lesion in the pvGPi.
B, Coronal image shows the relationship to the optic tract (*arrow*).
C, Sagittal image shows the surgical pallidotomy tracts (*arrows*) and the pallidotomy lesion (*arrowhead*).

nal intensity in the ipsilateral internal capsule and in the head of the caudate on T2-weighted images. Seven patients had hemorrhage along the probe tract. Of these, three had hematomas 2 to 3 cm in size within the surgical tract in the frontal lobe and four had hemorrhage involving the ipsilateral caudate, internal capsule, and putamen. Only one patient had significant mass effect, 5 mm of transfalcine herniation due to a large hematoma.

Follow-up images were obtained in three patients approximately 1 year after the pallidotomy procedure. Two had additional imaging because they underwent contralateral pallidotomy. In both, a very small (2–5 mm) focus of low signal on T1-weighted images and high signal on T2-weighted images was seen at the previous pallidotomy site. The postpallidotomy optic tract edema seen in one of these patients immediately after the procedure completely resolved on follow-up imaging. The third patient had no MR evidence of previous stereotactic intervention on follow-up images. No reason was given for follow-up imaging in this patient.

Discussion

In Parkinson disease, dopamine levels are decreased in the substantia nigra, putamen, and caudate nucleus (9, 10). The substantia nigra is the origin of the dopaminergic projection to the putamen. The putamen controls the activity of the pvGPi by direct and indirect pathways. In the direct pathway, in healthy patients, the putamen directly inhibits activity of the pvGPi. In patients with Parkinson disease, loss of dopamine causes a decrease in this inhibition, resulting in hyperactivity of the pvGPi. In the indirect pathway, loss of dopamine in the putamen results in hyperactivity of the subthalamic nucleus, which also causes hyperactivity of the pvGPi. The combined net effect is excessive inhibitory neuronal output from the pvGPi to the thalamocortical pathways, thought to be a major cause of bradykinesia (2, 3). Excessive inhibitory outflow by collaterals to the pedunculopontine nucleus may also account for various symptoms of Parkinson disease (4, 5). Posteroventral pallidotomy or localized destruction of the pvGPi interrupts this excessive inhibitory output from the basal ganglia (11–15) (Fig 6).

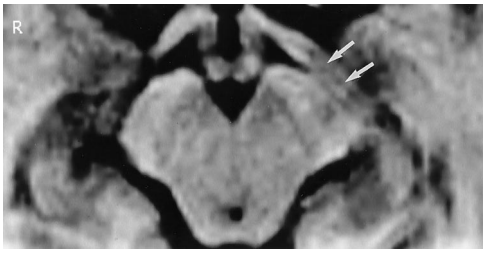

FIG 5. Axial volume-acquisition spoiled GRE image (33/11) with a flip angle of 35° 1 day after left-sided pallidotomy shows hypointensity extending into the left optic tract (*arrows*). The patient did not report a visual field deficit.

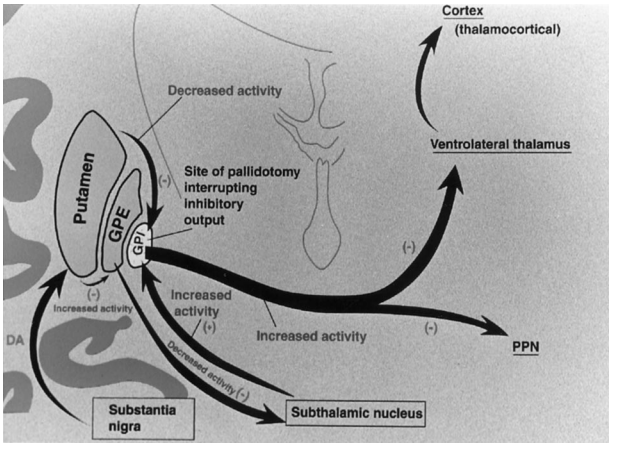

FIG 6. Diagram depicting the pathophysiology of Parkinson's disease. In the direct pathway, there is a relative decrease of inhibitory activity from the putamen to the pvGPi. In the indirect pathway, there is excessive inhibition of the GPe by the putamen, decreasing its inhibitory control on the subthalamic nucleus. The net result is increased inhibition of the ventrolateral thalamus (motor) and thalamocortical pathway as well as collaterals to the pedunculopontine nucleus (PPN). Pallidotomy disinhibits these pathways.

Although Parkinson disease was described over 150 years ago, significant progress in the treatment of this debilitating disease was not made until the late 1930s. During this period, Meyers (16, 17) performed open surgical interventions in the caudate nucleus, the basal ganglia, and the ansa lenticularis for the treatment of extrapyramidal diseases. The surgical treatment of extrapyramidal diseases became popular after the development of stereotactic surgery in 1947 (18). Six years later, a chemical pallidotomy, involving injections of procaine oil into the globus pallidus, was performed with a stereotactic headframe to treat Parkinson disease. In that series, patients remained free of symptoms for over 2 years (19).

In the 1950s Lars Leksell, a Swedish neurosurgeon, first performed electrocoagulation in the anterodorsal region of the internal portion of the GPi. Because of poor results, he changed his target to the posteroventral region of the GPi, and 95% of his patients showed improvement in the three cardinal signs of parkinsonism: tremor, rigidity, and bradykinesia (8). Despite these results, the pallidotomy was almost completely replaced by the thalamotomy, or localized surgical destruction of the thalamus (20).

With the advent of L-dopa pharmacotherapy, the surgical treatment of Parkinson disease was almost completely abandoned for all but the most severe cases of drug-resistant tremor. However, during the last 5 to 10 years, stereotactic operations have achieved a renewed significance in the treatment of Parkinson disease, owing in part to the realization that current pharmacotherapy has not been completely satisfactory. Medication intolerance, decreasing drug efficacy, and sometimes debilitating side effects, such as dyskinesia, may result in less than optimal outcomes (20, 21).

Advances in high-resolution imaging and in stereotactic neurologic surgery have made posteroventral pallidotomy a safe and accurate procedure (22). Furthermore, Laitinen et al (7) reported improvement in rigidity and hypokinesia in 92% of their patients and complete or almost complete relief of tremor in 81%. This confirmation of Leksell's surgical results has contributed to the reemergence of surgical treatment of Parkinson disease (19). Finally, advances in understanding the pathophysiology of this disorder have provided a scientific rationale for proceeding with surgical intervention. Parkinsonism experimentally produced in monkeys by using *N*-methyl-4 phenyl-1,2,3,6-tetrahydropyridine (MPTP) provides support for the efficacy of the pallidotomy procedure. Studies of the neural activity in these monkeys have shown neuronal hyperactivity in the GPi, which is the proposed cause of the excessive inhibitory activity in the thalamic and brain stem structures (23). Lesions introduced in areas that reduce pallidal output are effective in abolishing the signs of parkinsonism, thus providing a rationale for pallidotomy (24).

Our study shows a predictable radiologic appearance of the pallidotomy site, including its location and signal intensity. The large range in lesion size probably reflects adjustments in the pallidotomy technique, as several of the patients operated on early in our series had fewer passes and smaller lesions than did those whose procedures were done more recently. It is likely that the rim of hyperintensity on T2-weighted images represents edema. The procedure itself would be expected to elicit surrounding edema, and the resolution seen on the three follow-up studies would support that. Long-term follow-up with a larger population may confirm this hypothesis. The acute radio frequency thermocoagulation lesion causes denatured protein and cell death (25). The hyperintensity within the lesion seen on T1-weighted images immediately after surgery is probably due to a combination of coagulative neurons and blood.

High-resolution imaging played a vital role in the accurate determination of the pallidotomy site. Although not all patients had turbo spin-echo IR imaging, this sequence provided excellent resolution of the boundaries of the GPi, GPe, and lamina. Early experience suggests it is an important sequence for image-guided surgical planning. High-resolution postprocedural imaging studies are essential for assessing lesion location and size, and for delineating potential complications. Lesions placed only millimeters from the desired target may have vastly different long-term effects on parkinsonian motor signs (26).

Conclusion

All patients in this study experienced variable degrees of immediate improvement in contralateral bradykinesia, rigidity, and dystonia. Lesion location was so consistent that variations in location and outcome have not been studied. Immediately after surgery, the pallidotomy site showed a hyperintense or isointense center with a rim of hypointensity on T1-weighted and GRE images, a hypointense center with a hyperintense rim on T2-weighted images, and a hyperintense center with a hypointense rim on turbo spin-echo IR images. The volume of the pallidotomy lesions ranged from 52 to 264 mm^3 (average, 118 mm^3) and the midpoints of the lesion were located on average 3.5 mm anterior to the midcommissural point, 21 mm lateral to the middle aspect of the third ventricle, and 1.2 mm inferior to the midcommissural line.

References

1. Beal MF, Richardson EP, Martin JB. **Alzheimer's disease, parkensonism, and other degenerative disease of the nervous system.** In Wilson JD ed. *Harrison's Principles of Internal Medicine,* 12th ed. New York: McGraw-Hill; 1991:2065–2066
2. Delong MR. **Primate models of movement disorders of basal ganglia origin.** *Trends Neurosci* 1990;13:281–285
3. Eidelberg D, Moeller JR, Takikawa S, et al. **Brain metabolic topography in parkinsonism (abstract).** *Neurology* 1993;43(suppl 2): a270
4. Lacono RP, Shima F, Lonser RR, Kuniyoshi S, Maeda G, Yamada S. **The results, indications, and physiology of posteroventral pallidotomy for patients with Parkinson's disease.** *Neurosurgery* 1996; 36:1118–1125
5. Rye DB, Turner RS, Vitek JL, Bakay RAE, Crutcher MD, DeLong MR. **Anatomical investigations of the pallidotegmental pathway in monkey and man.** In: *The Basal Ganglia V.* New York: Plenum

Press; 1996:59–67
6. Starr PA, Vitek JL, Delong MR, Mewes K, Bakay RAE. **Pallidotomy: theory and techniques.** *Tech Neurosurg* (in press)
7. Laitinen LV, Bergenheim AT, Hariz MI. **Leksell's posteroventral pallidotomy in the treatment of Parkinson's disease.** *J Neurosurg* 1992;76:53–61
8. Svennilson E, Trovik A, Lowe R, Leksell L. **Treatment of parkinsonism by stereotactic thermolesions in the pallidal region: a clinical evaluation of 81 cases.** *Acta Psychiatr Neurol Scand* 1960;35:358–377
9. Hornykiewicz O, Kish SJ. **Biochemical pathophysiology of Parkinson's disease.** *Adv Neurol* 1986;45:19–34
10. Poirier L, Filion M, Langelier P, et al. **Brain nervous mechanisms involved in the so-called extra pyramidal motor and psychomotor disturbances.** *Prog Neurobiol* 1975;5:197–243
11. Kuo JS, Carpenter MB. **Organization of pallidothalamic projections in the rhesus monkey.** *J Comp Neurol* 1973;151:201–236
12. Kim R, Nakano K, Jayaraman A, et al. **Projections of the globus and adjacent structures: an autoradiographic study in the monkey.** *J Comp Neurol* 1976;169:263–290
13. DeVito JL, Anderson ME. **An autoradiographic study of efferent connections of the globus pallidus.** *Exp Brain Res* 1982;46:107–117
14. Harnois C, Filion M. **Pallidofugal projections to thalamus and midbrain: a quantitative antidromic activation study in monkeys and cats.** *Exp Brain Res* 1982;47:277–285
15. Parent A, DeBellefeuille L. **Organization of efferent projections from the internal segment of globus pallidus in primate as revealed by fluorescence retrograde labeling method.** *Exp Brain Res* 1982;245:201–213
16. Meyers R. **Surgical procedure for postcephalitic tremor, with notes on the physiology of the premotor fibers.** *Arch Neurol Psychiatry* 1940;44:455–459
17. Meyers R. **Surgical interruption of the pallidofugal fibres: its effect on the syndrome paralysis agitans and technical considerations in its application.** *NY State J Med* 1942;42:317–325
18. Spiegel EA, Wycis HT, Marks M, et al. **Stereotaxic apparatus for operations on the human brain.** *Science* 1947;106:349–350
19. Narabayshi H, Okuma T. **Procaine-oil blocking of the globus pallidus for the treatment of rigidity and tremor of parkinsonism.** *Proc Jpn Acad* 1953;29:134–137
20. Hassler R, Reichert T. **Indikationen und lokalisations methode der gezielten hirnoperationen.** *Nervenarzt* 1954;25:441–447
21. Marsden CD, Parkes JD, Quinn N. **Fluctuations of disability in Parkinson's disease: clinical aspects.** In: Marsden CD, Fahn S, ed. *Movement Disorders.* Boston: Butterworth Scientific; 1982:96–122
22. Lozano A, Hutchison W, Kiss Z, Tasker R, Davis K, Dostrovsky J. **Methods for microelectrode-guided posteroventral pallidotomy.** *J Neurosurg* 1996;84:194–202
23. Filion M, Tremblay L. **Abnormal spontaneous activity of globus pallidus neurons in monkey with MPTP-induced parkinsonism.** *Brain Res* 1991;547:142–151
24. Bergman H, Wichman T, Delong MR. **Reversal of experimental parkinsonism by lesions of the subthalamic nucleus.** *Science* 1990;249:1436–1438
25. Dieckman E, Gabriel E, Hassler R. **Size, form and structural peculiarities of experimental brain lesions obtained by thermocontrolled radiofrequency.** *Confin Neurol* 1965;26:134–142
26. Vitek JL, Bakay RAE, DeLong MR. **Microelectrode guided GPi pallidotomy for medically intractable Parkinson's disease.** *Adv Neurol* 1997;74:173–198

Please see the Editorial on page 1004 in this issue.